10th Xi'an ISL 2008

10TH INTERNATIONAL SYMPOSIUM ON LANDSLIDES AND ENGINEERED SLOPES

June 30 ~ July 4, 2008

Xi'an, China

Organized by

Chinese Institution of Soil Mechanics and Geotechnical Engineering, China Civil Engineering Society (CISMGE-CCES)
Chinese National Commission on Engineering Geology (CNCEG)
Chinese Society of Rock Mechanics and Engineering (CSRME)
Geotechnical Division of the Hong Kong Institution of Engineers (HKIE)

Supported by

China Geological Survey

Tsinghua University

China Institute of Water Resources and Hydropower Research (IWHR)

Inferences from morphological differences in deposits of similar large rockslides.
A.L. Strom
Geotechnical analysis of a complex slope movement in sedimentary successions of the southern Apennines (Molise, Italy)
D. Calcaterra, D. Di Martire, M. Ramondini, F. Calò, M. Parise
Pir3D , an easy to use three dimensional block fall simulator
Y. Cottaz
Characterization of the fracture pattern on cliff sites combining geophysical imaging and laser scanning
J. Deparis
In situ characterization of the geomechanical properties of an unstable fractured rock slope
C. Dünner, P. Bigarré,F. Cappa , Y. Guglielmi,C. Clément
Stability problems in slopes of Arenós reservoir (Castellón, Spain)
J. Estaire, J. A. Díez, C. Olalla
"The 22 August, 2006, anomalous rock fall along the Gran Sasso NE wall (Central Apennines, Italy)"
G. Bianchi Fasani, C. Esposito, G. Scarascia Mugnozza, L. Stedile, M. Pecci

16:20 – 18:20 Oral presentation 30 June 2008 Monday
Parallel Session 1B-1: Advance in analytical methods, modelling and prediction of slope behavior (B)
Venue: ROOM 4-1 OF BUILDING NO. 10
Chairpersons: *Keizo Ugai, N Rosser*

Probability limit equilibrium and distinct element modeling of jointed rock slope at northern abutment of Gotvand dam, Iran
M. Aminpoor, A. Noorzad & A.R. Mahboubi
Contribution to the safety evaluation of slopes using long term observation results
J. Barradas
Delimitation of safety zones by finite element analysis
J. Bojorque , G. De Roeck G. De Roeck & J. Maertens
Superposition principle for stability analysis of reinforced slopes and its FE validation
F. Cai, K. Ugai
Soil suction modelling in weathered gneiss affected by landsliding
M. Calvello, L. Cascini, G. Sorbino, G. Gullà
"Modelling the transient groundwater regime for the displacements analysis of slow-moving active landslides"
L. Cascini, M. Calvello, G.M. Grimaldi
Numerical modelling of the thermo-mechanical behaviour of soils in catastrophic landslides
F. Cecinato, A. Zervos, E. Veveakis & I. Vardoulakis
Slope stability analysis using graphic acquisitions and spreadsheets
L. H. Chen, Z. Y Chen, Ping Sun
Efficient evaluation of slope stability reliability subject to soil parameter uncertainties using importance sampling
Jianye Ching, Kok-Kwang Phoon, Yu-Gang Hu

Landslides and Engineered Slopes – Chen et al. (eds)
© 2008 Taylor & Francis Group, London, ISBN 978-0-415-41196-7

Delimitation of safety zones by finite element analysis

J. Bojorque, G. De Roeck & J. Maertens
Dept. of Civil Engineering, K.U. Leuven, Leuven, Belgium

ABSTRACT: This paper deals with the determination of safety zones and local minima by using finite element analysis. Used is made of finite element method in order not to constraint the analysis by neither the assumptions in the location of the sliding surface nor in the interslice force function. It is known, that only the most critical failure mechanism and global minimum are evaluated by the strength reduction method, in such approach local minima most of the time are unnoticed. Here, it is proposed that the safety zones and the local minima can be detected by keeping the information generated in the strength reduction process. In addition, the importance of soil properties in the location of the failure mechanism is highlighted. The methodology is presented in an artificial case study and in a real natural slope. The safety zones should be considered in landslide stabilization and remediation.

1 INTRODUCTION

Numerical methods have been recognized as a powerful tool for practical geotechnical applications. These techniques have become important for slope stability analysis, especially when complex stratigraphy and complex soil behaviour are treated. Moreover, the use of the strength reduction method (SRM) to define the stability of a slope has shown some advantages over traditional methods (Griffiths & Lane 1999, Dawson & Drescher 1999), among others. On the other hand, one limitation of the strength reduction approach is that only the most critical failure mechanism and global minimum are evaluated (Cala et al. 2004; Cheng et al. 2007). Therefore, by SRM, local minima most of the time are unnoticed. In engineering practice apart from the global factor of safety and the critical sliding surface associated with it, it is important to detect the local minima.

In classical limit equilibrium analysis, local minima are defined by evaluating different sliding surfaces associated with different safety factors. A single line to characterize the sliding mechanism can mislead the implementation of remedial measures. Safety maps can be generated by using limit equilibrium concepts to detect safety/unsafety areas. Those maps are represented by a series of contour lines along which minimal safety factors are constant (Baker & Leshchinsky 2001, Renaud et al. 2003). However, limit equilibrium methods need to use key assumptions in other to solve the problem. These assumptions and the disregard of the strain-stress relationship limit their use in some extension.

The modified shear strength reduction technique in the framework of Finite Difference Method (Cala et al. 2004), has been proposed in order to detect several sliding surfaces. The technique is based on gradually reducing the strength properties after identification of the first sliding surface. The modified technique needs extra computations and is not applicable for finite element analysis, causing some numerical problems. In this paper, it is proposed that the strength reduction technique used in the framework of finite element method can still given information regarding different failure mechanisms by keeping the different stages generated during the process. Furthermore, the necessity of detect different failure mechanisms that can arise from small changes in soil parameters is highlighted. Used is made of finite element methods in order not to constraint the analysis by neither the assumptions in the location of the sliding surface nor in the interslice force function. Moreover, the advantages of finite element slope stability analysis can be exploited.

Safety zones and local minima are detected in finite element analysis by keeping all the shear zones defined by using different strength reduction coefficients (Bojorque et al. 2007). The safety zones should be considered for the selection and location of remedial measures for landslide stabilization. The verification of the procedure is presented in an artificial case study acquired form literature in which the development of local minima is indicated. The methodology is implemented, as well, in a case study of a natural slope located in Ecuador where the presence of different failure mechanisms should be evaluated.

2 FINITE ELEMENT METHOD—STRENGTH REDUCTION TECHNIQUE

In the framework of finite element slope stability analysis, the Factor of Safety (FoS) is defined as classical methods. Hence, the factor of safety of a slope is defined as the factor by which the shear strength parameters must be divided in order to bring the slope to failure (Griffiths and Lane 1999). When the same strength reduction factor (SRF) is used for both, the cohesion (c) and tangent of the friction angle ($\tan\phi$), Equation 1 holds.

$$SRF = \frac{c}{c_f} = \frac{\tan\phi}{(\tan\phi)_f} \tag{1}$$

where c_f and $(\tan\phi)_f$ represent the factored parameters.

To compute the factor of safety and its associated failure mechanism, finite element method uses the strength reduction method (SRM). In this process, the *cohesion* and $\tan\phi$ are gradually reduced or increased until non-convergence or convergence, respectively, in the plastic solution is found. This reduction or increase will depend on both, the initial estimation of the strength reduction factor and the stability of the slope. When small changes in the strength reduction factor produce jumps from convergence to non-convergence in the solution, the factor of safety is determined. At this limit, Equation 1 can be re-written as,

$$\text{SRF at failure} = \text{Factor of Safety} = \frac{\text{available strength}}{\text{critical strength}} \tag{2}$$

It is noticed, based on Equation 2, that if the initial estimation of the safety factor, represented by SRF, is higher than the factor of safety, the SRM will reduce the soil strength parameters by increasing the estimated SRF. Otherwise, if the initial estimation is lower than the factor of safety, the approach needs to increase the strength parameters.

Before performing the SRM, the initial state of stress should be determined. For cases where the slope is stable, FoS ≥ 1, the initial state of stress is normally computed by the gravity loading procedure using the slope own-weight. On the contrary, when the slope is unstable, FoS < 1, the K0-procedure is adopted, with a typical value of $K0 = 1-\sin\phi$. In this last approach, the vertical stress (σ_v) is determine by the weight of the slope and the horizontal stress (σ_h) is obtained from the relationship $K0 = (\sigma_h/\sigma_v)$. Once the initial stresses are computed, the determination of the factor of safety is obtained by the SRM. The SRM will process different calculations for different strength parameters (strength reduction factor), some of them will be higher than the factor of safety and other lower than this value. By retaining and properly visualization of the different steps, it is possible to detect other failure surfaces that can emerge from the computations. The failure mechanism can be identified by the shear strain contour computed from the results of the SRM. Different failure mechanisms associated with different reduced parameters can be detected and incorporated in safety zones by locating different shear zones (Bojorque et al. 2007).

The finite element program PLAXIS using 15-node elements is used for the slope stability analysis based on the strength reduction method (PLAXIS-BV 2004). The soils are modelled as elastic-plastic material with Mohr-Coulomb failure criterion and zero-tensile strength. Vertical and horizontal displacements restricted on the base and horizontal displacements restricted on the sides are used as boundary conditions for the analyses.

3 NUMERICAL EXAMPLE

A two slope angles example is presented to compute the safety zones. The geometrical configuration and soil properties are given in Figure 1. This example is taken from the benched slope case presented in (Cala et al. 2004). The lower slope is inclined 45° and the upper one is inclined 40°.

3.1 *Limit equilibrium safety map*

A comparative analysis is presented with respect to limit equilibrium calculations in order to validate the results. Bishop's limit equilibrium equations using circular slip surface is adopted. Figure 2 shows the critical sliding surface determined by Bishop's method. Besides, the location of the 100 most unsafe slip surfaces are given.

It is worth noticing that two well defined failure mechanisms are presented. One located in the lower slope, in which the critical slip surface is developed

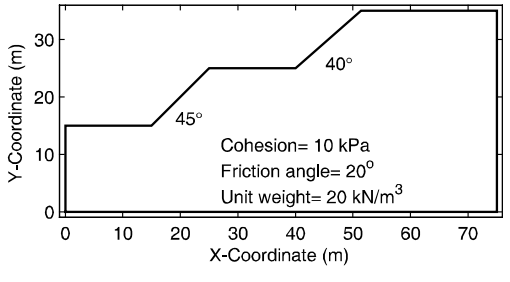

Figure 1. Geometrical configuration and soil properties of the two-angle slope example.

and has a safety factor, associated with it, equal to 0.94. The other mechanism is located in the upper slope with a minimum safety factor corresponding to 0.99. The first 100 sliding surfaces corresponded to factors of safety from 0.94 to 1.06. A better representation of the limit equilibrium results can be given by a safety map (Baker and Leshchinsky 2001; Renaud et al. 2003).

The safety map is constructed by dividing the slope model by a mesh and assigning to each point in a mesh a factor of safety obtained by minimizing the factor of safety between all the slip surfaces going through this point (Renaud et al. 2003). For this example the slope is divided into a rectangular mesh instead of a triangular mesh. For each point in the grid the minimum factor of safety from the nearest slip surface is input. Any limit equilibrium method can be used for the computation of the sliding surfaces, for this example Bishop's method with circular slip surfaces is used. A rectangular mesh spacing of 0.15 m is adopted for the discretization. A filtering value of 1.4 in the safety factor is used to enhance the visualization of the safety map. Figure 3 shows the safety map for the two slope angles example and the critical slip surface is represented by the white hashed line which correspond a factor of safety equal to 0.94.

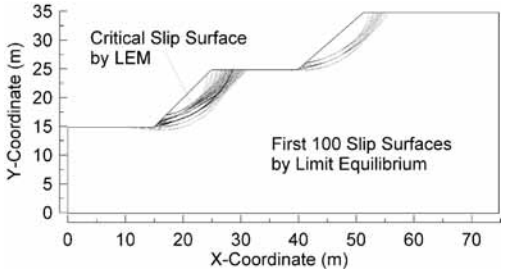

Figure 2. Critical and first 100 most unsafe slip surfaces generated by Bishop's limit equilibrium method. Factor of safety for the critical slip surface equal to 0.94.

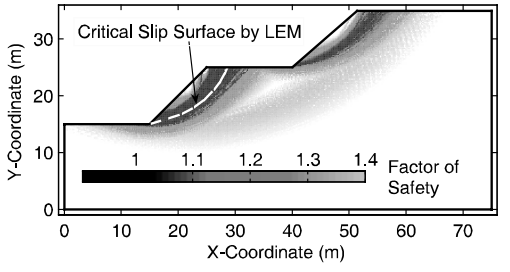

Figure 3. Safety map generated from Bishop's limit equilibrium method. Critical slip surface (white hashed line) correspond to a factor of safety equal to 0.94.

The darker zones are critical areas where the failure can occur. This map is generated by using 10, 000 circular slip surfaces. From this map the determination of safety zones are enhanced by retaining and visualizing all slip surface information.

3.2 *Finite element results*

For the two slope angles example the FoS determine by FE-SRM is equal to 0.87. This value was computed by performing 60 steps in the SRM. It is noticed that after the fourth step, the critical factor of safety has been reached, the next computations from 5 to 60, are performed to check the stability of the SRM. From step 4 to the last step 60, the plastic points are constant and are located at the lower slope (Fig. 4b). In stage 3, when the strength reduction factor is equal to 0.93, two failure mechanisms are detected (Fig. 4a). If only the last result is considered, as it is typically the case, the second mechanism at the upper slope is unnoticed. This can mislead the implementation of remedial measures. Therefore, the slope stability performance for others strength reduction factors is needed.

In PLAXIS, the initial SRF is computed automatically, this can be a drawback if others values are needed

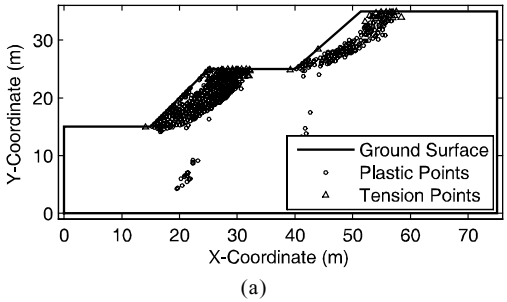

(a)

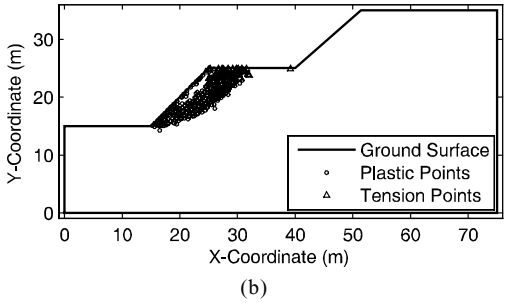

(b)

Figure 4. Plastic and tension points generated during the strength reduction method. (a) Stage 3, strength reduction factor equal to 0.93. (b) Stage 4, strength reduction factor equal to 0.88.

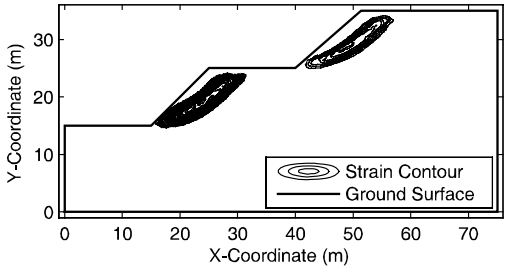

Figure 5. Shear strain contour generated during the strength reduction method at Stage 4, strength reduction factor equal to 0.88.

to be check. For this example, the initial SRF value is 1.03, for step 2 the SRF is reduced to 0.98, and in stage 3 to 0.93. For the example, these SRF values are adequate to detect different potential failures.

When performing a FE-SRM, it is necessary to retain all the different strength reduction computations. This information enables to detect potential unstable mechanisms. By exporting the strains generated at the Gauss points and drawing the shear strain contour for different limits, others failure mechanisms can be detected. Figure 5 shows the shear strain contour computed for stage 4, from this stage and on, plastic points are not more generated at the upper slope (Fig. 4b). By the properly vizualization the location of the two failure zones and the potential unstable zones are located. By this process it is plausible to detect different safety zones in which adequate stabilization measures can be implemented.

Good correspondence between limit equilibrium results (Figs. 2–3) and SRM (Fig. 5) are produced. The safety map generated by Bishop's limit equilibrium method and the safety zones determined by the shear strain contour shows the same failure mechanisms.

For simple slope problems, the determination of safety zones, by shear zones or safety map, is less critical since the critical sliding mechanism and local minima are near to each other. Any slope stabilization action done for the most critical failure mechanism will affect the other mechanisms. The local minima will fall inside the shear strain contour and plastic points developed by FE-SRM. Therefore, it facilitates the slope stability analysis.

4 INFLUENCE OF SOIL PROPERTIES

In this second example, the importance of considering different soil parameters in the failure location is shown. This example is a slope located at km 27+000 at the left hand side of the road Cuenca-Machala in Ecuador. It has an inclination of about 40 degrees. Three main soil units are identified; colluvium, weathered tuff material (Tuff) and the volcanic rock basement. The stratigraphy and cross-section configuration are shown in Figure 6. Soil mechanical parameters are given in Table 1, in which, γ is the unit weight, c is the cohesion, ϕ is the friction angle, E represents the Young's modulus, and ν is the Poisson's ratio. For all the analyses zero-tensile strength is used. Soil parameters were obtained from performing in situ and laboratory tests.

For the colluvium stratum, in which the potential landslide is situated, the cohesion has a value between 9 to 15 kPa and the friction angle varies from 23 to 29°. Even tough, the relative small variation in soil parameters, this changes the location of the failure surface. Figure 7a shows the shear strain contour for the slope having a $c = 9$ kPa and $\phi = 29°$, for those parameters the FoS is equal to 1.27 and the failure surface indicated by the strain contour is located at the upper part of the colluvium. For the same geometrical configuration and by changing the c to 10 kPa and ϕ to 26°, a second failure mechanism arises, this second failure is deeper and it is located at the lower part of the stratum (Fig. 7b). For this case, the computed FoS is equal to 1.19. If now, the $c = 15$ kPa and $\phi = 23°$, the upper failure disappears and only the lower failure is detected (Fig. 7c), having a FoS equal to 1.14.

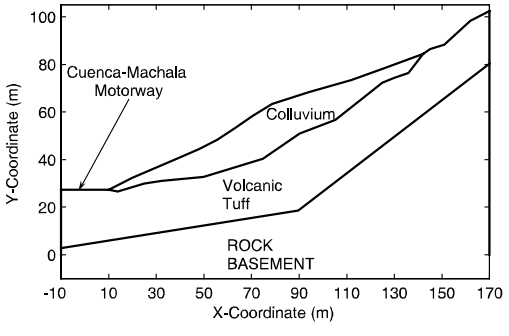

Figure 6. Stratigraphy and geometrical configuration for the potential instability at Cuenca-Machala motorway (km 27+000), Ecuador.

Table 1. Geomechanical properties for the different materials.

Parameter symbol	Units	Colluvium	Material tuff	Rock
γ	kN/m^3	16.7	17.6	24.5
c	kPa	9–15	60.0	200
ϕ	degrees	23–29	33.5	40.0
E	MPa	60	100	300
ν	[-]	0.25	0.25	0.40

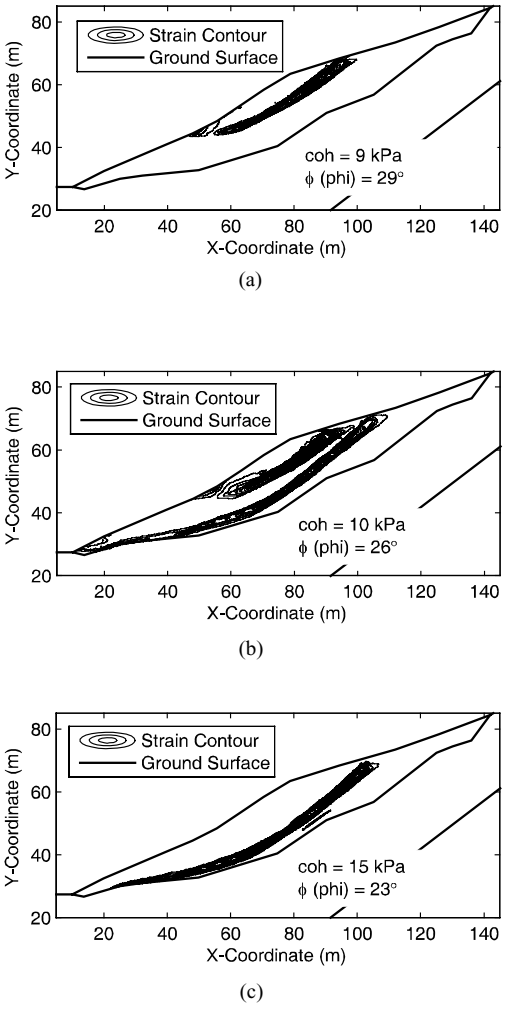

Figure 7. Shear strain contours generated during the strength reduction method. (a) upper failure, $c = 9$ kPa and $\phi = 29°$, factor of safety equal to 1.27. (b) mixed failure, $c = 10$ kPa and $\phi = 26°$, factor of safety equal to 1.19. (c) lower failure, $c = 15$ kPa and $\phi = 23°$, factor of safety equal to 1.14.

This example shows that for small different soil strength parameters very different failure mechanisms can be developed. To construct safety zones the location of the different failures should be delimitated.

It is worth noticing that by the principal of the strength reduction method, all slopes which have the same strength parameters (c and $\tan\phi$) but are factored by any scalar, will have the same failure mode. In other words, if a slope has parameters c_1, $\tan\phi_1$ and FoS_1, then, if another slope has parameters $c_2 = c_1^* F$ and $\tan\phi_2 = \tan\phi_1^* F$, then the factor of safety FoS_2 is equal to $FoS_1^* F$, and the failure mechanisms is the same. In which, F is any scalar number. This definition is valid for cases where no external load or water forces are presented. Taking this relationship into account, a plot can be draw indicating some of the combination of the soil parameters (c and $\tan\phi$) that will have the same failure mechanism. Figure 8 shows the combination of cohesion, $\tan\phi$ and ϕ, which gives the same failure mechanism and where the factor of safety will be ratio to each other.

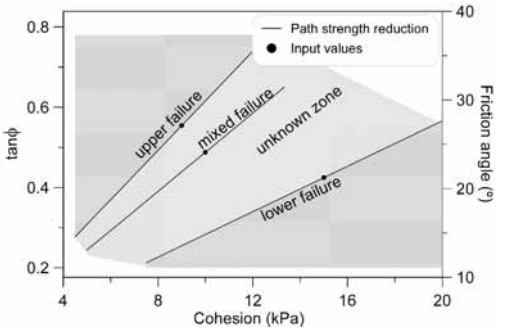

Figure 8. Delimitation of different failure modes depending in soil properties combinations.

The upper, mixed and lower lines represent the factored parameters (c and $\tan\phi$). All the strength parameter combinations that fall above the upper failure line will produce an upper failure. And all the combinations that fall below the lower failure will develop a lower failure. At the "unknown zone" (lack of computations), if the parameters are above the mixed failure line, the failure can be mixed or upper, if the parameters fall below the later line the failure will be mixed or lower. The exact limits between the different mechanisms are not yet defined, further research is still going on to define these limits and reduce the unknown zone.

5 CONCLUSIONS

This study presents a proposal to identify different failure surfaces by retaining the information given in the strength reduction method by different strength reduction factors. Finite element method is used in order not to constraint the analysis by the assumptions employed by others methods regarding the failure. By properly vizualization of the shear strain contour the safety zones are detected. The strength reduction factor used to compute the factor of safety gives local minima for different computations. Good agreement is encountered with the safety map generated by limit equilibrium method.

Small changes in soil properties can cause remarkable changes in the failure mechanism, thus safety zones should be evaluated by performing different soil combinations. By appropriately manipulation of the finite element slope stability information, the full extent of potential slope instability is depicted. This will contribute for the correct design and implementation of the stabilization measures.

ACKNOWLEDGEMENTS

The first author would like to thank for the financial support provided by the K.U. Leuven in the context of the Selective Bilateral Agreement between K.U. Leuven and Latin America.

REFERENCES

Baker, R. & D. Leshchinsky. 2001. Spatial distribution of safety factors. *Journal of geotechnical and geoenvironmental engineering* 127(2), 135–145.

Bojorque, J., G. De Roeck & J. Maertens. 2007. Comments on two-dimensional slope stability analysis by limit equilibrium and strength reduction methods by Cheng *et al. doi:10.1016/j.compgeo.2007.04.005* (in press).

Cala, M., J. Flisiak & A. Tajdus. 2004. Slope stability analysis with modified shear strength reduction technique. In W. Lacerda, M. Erlich, S. Fontoura, and A. Sayao (Eds.), *Proc. 9th intern. symp. on Landslides*; *Landslides: Evaluation and Stabilization, Rio de Janeiro, Brazil.*

Cheng, Y.-M., T. Lansivaara & W.-B. Wei. 2007. Two-dimensional slope stability analysis by limit equilibrium and strength reduction methods. *Computers and Geotechnics* 34(3), 137–150.

Dawson, E. & W. Drescher. 1999. Slope stability analysis by strength reduction. *Géotechnique* 49(6), 835–840.

Griffiths, D. & P. Lane. 1999. Slope stability analysis by finite elements. *Géotechnique* 49(3), 387–403.

PLAXIS-BV. 2004. 2d-version 8, finite element code for soil and rock analysis. *Slope Stability Analysis, Delft University of Technology and Plaxis, The Nederlands.*

Renaud, J.-P., M. Anderson, P. Wilkinson, D. Lloyd & D. Muir-Wood. 2003. The importance of visualization of results from slope stability analysis. *Proceedings ICE, Geotechnical Engineering* 156, 27–33.